PAPER • OPEN ACCESS

Quantum circuit optimization for arbitrary high-dimensional bipartite quantum computation

To cite this article: Gui-Long Jiang and Hai-Rui Wei 2026 *New J. Phys.* **28** 044502

New Journal of Physics
The open access journal at the forefront of physics

Deutsche Physikalische Gesellschaft DPG
IOP Institute of Physics

Published in partnership with: Deutsche Physikalische Gesellschaft and the Institute of Physics

PAPER

Quantum circuit optimization for arbitrary high-dimensional bipartite quantum computation

Gui-Long Jiang[1,2] **and Hai-Rui Wei**[1,*]

[1] School of Mathematics and Physics, University of Science and Technology Beijing, Beijing 100083, People's Republic of China
[2] School of Mathematics, Harbin Institute of Technology, Harbin 150001, People's Republic of China
[*] Author to whom any correspondence should be addressed.

E-mail: hrwei@ustb.edu.cn

Keywords: quantum computation, quantum circuit, universal quantum gate

OPEN ACCESS

RECEIVED
9 October 2025

REVISED
15 February 2026

ACCEPTED FOR PUBLICATION
23 March 2026

PUBLISHED
2 April 2026

Abstract

Implementation of high-dimensional (HD) quantum gates shows very promising perspectives for HD quantum computation. A bipartite quantum system with arbitrary dimensions n and m is termed a quNit–quMit. Here we propose a synthesis scheme to construct the quantum circuit for general quNit–quMit gates with controlled increment (CINC) gates and local gates. This shows that CINC gates combined with local gates form a universal gate set for HD quantum computation. An upper bound of $O(n^2)$ CINC gates is achieved for arbitrary quNit–quMit gate implementation in the proposed scheme, which is the best known result. Especially for the controlled quNit–quMit gates, our scheme requires only 2 CINC gates, whereas the previous scheme required $2n$.

1. Introduction

A high-dimensional (HD) quantum system, called qudit (d-level with $d>2$), gradually exhibits remarkable advantages over binary systems in quantum information processing, due to its higher information capacity [1], better security against eavesdropping [2, 3], and boosted algorithmic efficiency [4–6]. The physical qudit platforms have been naturally achieved in photonic systems [7, 8], continuous spin systems [9], ion traps [10, 11], and superconducting circuits [12–14]. Up to now, qudit-based quantum communication tasks have been studied both theoretically and experimentally, including quantum key distribution [15–17], quantum teleportation [18–20], and quantum cryptography [2, 21]. In the field of qudit-based quantum computing, quantum algorithms [4, 6], quantum error correction [22, 23], and HD quantum gates [24–33] have been widely discussed. By employing accessible qudits, qubit-based circuit size, depth (the number of time steps required for quantum operations), and complexity (the number of elementary gates required for the quantum computation) might be further reduced, and the experimental setup for realizing qubit gates can be greatly simplified [34–38].

It is impractical to construct a different physical setup for the realization of each multi-qudit operation. A natural idea is to decompose arbitrary quantum operations into a sequence of simple-to-perform quantum gates. A set of quantum gates is called a universal gate set if any quantum operation can be synthesized from the gates in the set. It is well known that single-qubit gates and controlled-NOT (CNOT) gates together form a universal gate set for multi-qubit computing [39]. For multi-qudit computing, the collection of single-qudit gates together with a two-qudit *imprimitive* gate that maps a certain product state to an entangled state is a universal gate set [40]. Some imprimitive gates for qudits, such as controlled-double-NOT (CDNOT) gates [38], generalized controlled X (GCX) gates [41], and controlled increment (CINC) gates [42], have been used to construct quantum circuits for implementing any multi-qudit operation. A bipartite imprimitive gate is more difficult to realize than a local gate, as it is generally more susceptible to environmental noise. This motivates using imprimitive gate counts to quantify the cost of a quantum circuit.

Optimizing the circuit cost is important as it reduces the circuit operation time and the probability of gate errors occurring. For n-qutrit (3-level) systems, the current least-cost scheme requires $\frac{41}{96}\cdot 3^{2n}-4\cdot 3^{n-1}-(\frac{n^2}{2}+\frac{n}{4}-\frac{29}{32})$ GCX and CINC gates to synthesize a general n-qutrit gate [43].

However, this scheme uses two types of imprimitive gates. For n-ququart (4-level) systems, Li *et al* [38] proposed a scheme to construct a quantum circuit of general n-ququart gates, where $5(4^{2(n-1)}-4^{n-1})$ CDNOT gates are required. The theoretical lower bound of $[d^{2n}-n(d^2-1)-1]/[4(d-1)]$ GCX gates for implementing a general n-qudit gate was derived by Di and Wei [44]. However, no existing synthesis scheme has achieved the lower bound. Several techniques of matrix decomposition are used to construct quantum circuits, such as quantum Shannon decomposition (QSD) [38, 41], QR decomposition [42], cosine–sine decomposition (CSD) [44, 45], spectral decomposition [46], and Cartan decomposition [43, 47]. In these synthesis schemes [38, 41–43, 45], any two-qudit gate is first decomposed into a sequence of the given imprimitive gates and single-qudit gates, and then any n-qudit gate is decomposed into two-qudit and single-qudit gates. Thus, a quantum circuit for implementing general two-qudit gates is important because its cost significantly affects the overall circuit cost. For qubits, the minimal cost of quantum circuits for implementing general two-qubit gates is 3 CNOTs [48]. For qudits, the minimal circuit cost for implementing general two-qudit gates remains an open challenge.

Here we focus on designing the quantum circuit for general quNit–quMit unitary operations with arbitrary dimensions n and m. In the paper, we choose a set that includes all single-qudit gates and a CINC gate as a universal gate set. We first accurately implement a quNit–quMit controlled unitary gate using local gates and two CINC gates, and a quantum circuit for HD uniformly controlled unitary gates is constructed in section 3. Subsequently, using CSD, we propose a synthesis scheme to construct the quantum circuit for general quNit–quMit gates in terms of CINC gates and local gates in section 4. In contrast to the synthesis schemes using GCX [41, 43, 44], our approach requires only a single type of CINC gate. The controlled systems of all CINC gates in the quantum circuit are located on the same subsystem. The number of universal gates required for our HD quantum circuits is the lowest currently known (see table 1), with detailed calculations provided in section 5. The proposed synthesis scheme is not dependent on the physical platform. As long as a physical system can realize CINC gates and local gates, the arbitrary HD quantum computation can be achieved according to our scheme.

2. The concepts of HD quantum gates

2.1. HD quantum gates on single systems

Let $\mathcal{H}_n$ be an n-dimensional quantum state space and $\{|1\rangle,\ldots,|n\rangle\}$ be an orthonormal basis of $\mathcal{H}_n$. Throughout the paper, the letters i, j, k, and l denote positive integers. The identity operator $\sum_{i=1}^{n}|i\rangle\langle i|$ on $\mathcal{H}_n$ is denoted by I_n. For $1\leqslant i<j\leqslant n$, define three types of $n\times n$ Hermitian matrices as follows:

$$\sigma_{z_n}^{ij}=|i\rangle\langle i|-|j\rangle\langle j|,\ \ \sigma_{x_n}^{ij}=|i\rangle\langle j|+|j\rangle\langle i|,\ \ \sigma_{y_n}^{ij}=-\mathrm{i}|i\rangle\langle j|+\mathrm{i}|j\rangle\langle i|. \tag{1}$$

A $(i,j;\varphi_n,\theta)$-rotation gate on $\mathcal{H}_n$ is defined as [41]

$$R_{\varphi_n}^{ij}(\theta)=\exp\left(-\mathrm{i}\frac{\theta}{2}\sigma_{\varphi_n}^{ij}\right), \tag{2}$$

where $1\leqslant i<j\leqslant n$, $\varphi\in\{x,y,z\}$, and the rotational parameter $\theta\in[0,2\pi]$. It is a natural generalization of φ-axis rotation gates on a single qubit [49], as the action of $R_{\varphi_n}^{ij}(\theta)$ is to perform a φ-axis rotation gate with a rotational parameter θ on the two-dimensional state space spanned by $\{|i\rangle,|j\rangle\}$. In addition, the $(i,j;\varphi_n,\theta)$-rotation gate can be physically implemented by using Mach–Zehnder interferometers [50, 51].

A generalized Pauli-X operator on $\mathcal{H}_n$ is defined as [29]

$$X_n=|1\rangle\langle n|+\sum_{i=1}^{n-1}|i+1\rangle\langle i|. \tag{3}$$

When $n=2$, the operator above is equal to the Pauli-X (NOT) gate on a single qubit. The operator X_n is also known as an increment gate, and $n-1$ powers of X_n is equal to its conjugate transpose, i.e. $X_n^{\dagger}=X_n^{n-1}$. Hereafter, $\dagger$ denotes the conjugate transpose operation. We define a unitary operator T_n on $\mathcal{H}_n$ as

$$T_n=|1\rangle\langle 1|+\sum_{i=2}^{n}|i\rangle\langle n+2-i|. \tag{4}$$

It holds that

$$T_n^{\dagger}=T_n,\ \ T_n\cdot X_n\cdot T_n=X_n^{\dagger}. \tag{5}$$

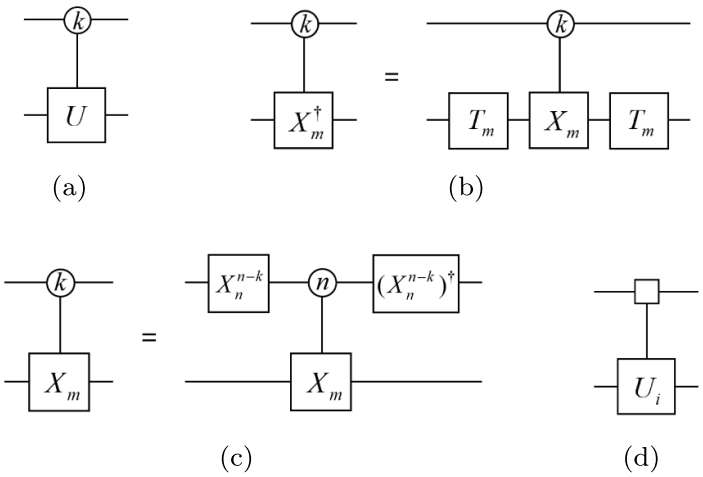

Figure 1. Quantum circuit symbols. (a) Controlled unitary gate with the control system state $|k\rangle_1$. The circle represents the control system. (b) Relation between $\mathrm{C}_k(X_m^\dagger)$ and $\mathrm{C}_k(X_m)$. (c) Relation between $\mathrm{C}_n(X_m)$ and $\mathrm{C}_k(X_m)$. (d) Uniformly controlled unitary gate with the control system $\mathcal{H}_n^1$. The square (□) denotes the control system.

2.2. HD quantum gates on bipartite systems

We write $\mathcal{H}_n^1 \otimes \mathcal{H}_m^2$ to denote a bipartite quantum system composed of an n-dimensional state space $\mathcal{H}_n^1$ and a m-dimensional space $\mathcal{H}_m^2$. Let $\{|i\rangle_1 | 1 \leqslant i \leqslant n\}$ and $\{|j\rangle_2 | 1 \leqslant j \leqslant m\}$ be orthonormal bases of $\mathcal{H}_n^1$ and $\mathcal{H}_m^2$, respectively. The subscripts of $|i\rangle_1$ and $|i\rangle_2$ are omitted, and the notation $|i\rangle$ is used when the context clearly distinguishes between the first and second quantum systems.

An operator on $\mathcal{H}_n^1 \otimes \mathcal{H}_m^2$ is said to be a controlled unitary gate with the control system state $|k\rangle_1$, if its action is to perform a specific unitary operator on the target system $\mathcal{H}_m^2$ when the state of $\mathcal{H}_n^1$ is $|k\rangle_1$; otherwise, it does nothing. The mathematical representation of the controlled unitary gate with the control system state $|k\rangle_1$ can be written as

$$\mathrm{C}_k(U) = |k\rangle\langle k| \otimes U + \sum_{i=1, i\neq k}^{n} |i\rangle\langle i| \otimes I_m, \tag{6}$$

where U is a unitary operator on $\mathcal{H}_m^2$ and I_m is the identity operator on $\mathcal{H}_m^2$. Its quantum circuit is given in figure 1(a). Equation (6) implies the following properties

$$\begin{aligned} &\mathrm{C}_k\left(U^\dagger\right) = \left(\mathrm{C}_k(U)\right)^\dagger, \\ &\mathrm{C}_k(UV) = \mathrm{C}_k(U) \cdot \mathrm{C}_k(V), \\ &\mathrm{C}_k(U) \cdot \mathrm{C}_l(V) = \mathrm{C}_l(V) \cdot \mathrm{C}_k(U), \\ &\mathrm{C}_k\left(VUV^\dagger\right) = I_n \otimes V \cdot \mathrm{C}_k(U) \cdot I_n \otimes V^\dagger \end{aligned} \tag{7}$$

for every $k \neq l \in \{1, \ldots, n\}$ and any two unitary operators U and V on $\mathcal{H}_m^2$.

Particularly, when $U = X_m$ in equation (6), it is defined as a controlled-X_m (i.e. CINC) gate [33]

$$\mathrm{C}_k(X_m) = |k\rangle\langle k| \otimes X_m + \sum_{i=1, i\neq k}^{n} |i\rangle\langle i| \otimes I_m. \tag{8}$$

From equations (5) and (7), it holds that

$$\begin{aligned} \mathrm{C}_k\left(X_m^\dagger\right) &= \mathrm{C}_k(T_m \cdot X_m \cdot T_m) \\ &= I_n \otimes T_m \cdot \mathrm{C}_k(X_m) \cdot I_n \otimes T_m. \end{aligned} \tag{9}$$

Equation (9) means that $\mathrm{C}_k(X_m^\dagger)$ is equivalent to $\mathrm{C}_k(X_m)$ up to two local unitary operators T_m, as shown in figure 1(b). Moreover, $\mathrm{C}_k(X_m)$ can be transformed into $\mathrm{C}_n(X_m)$ by local gates on $\mathcal{H}_n^1$, as shown in figure 1(c).

When the control system is a qubit (i.e. $\mathcal{H}_2^1 \otimes \mathcal{H}_m^2$), $\mathrm{C}_1(X_m)$ or $\mathrm{C}_2(X_m)$ can be experimentally realized effectively using only linear optical elements and the polarization degree of freedom of photons

[33, 52]. However, for $\mathcal{H}_n^1 \otimes \mathcal{H}_m^2$ where $n > 2$, it is extremely difficult to implement $\mathrm{C}_k(X_m)$ solely using the photonic polarization, as photonic polarization is inherently insufficient to encode more than a two-level system. Although this is not directly relevant to the main results of this paper, for the sake of completeness, we provide an experimental implementation of $\mathrm{C}_n(X_m)$ where $n > 2$ in appendix A.

The operator $\mathrm{C}_k(U)$ may be generalized as follows. Let $\{U_1, \ldots, U_n\}$ be a unitary operator set on $\mathcal{H}_m^2$. A uniformly controlled unitary gate with the control system $\mathcal{H}_n^1$ is defined as

$$\sum_{i=1}^{n} |i\rangle\langle i| \otimes U_i = \begin{bmatrix} U_1 & \mathbf{0} & \cdots & \mathbf{0} \\ \mathbf{0} & U_2 & \cdots & \mathbf{0} \\ \vdots & \vdots & \ddots & \vdots \\ \mathbf{0} & \mathbf{0} & \cdots & U_n \end{bmatrix}. \tag{10}$$

The action of such a gate on $\mathcal{H}_n^1 \otimes \mathcal{H}_m^2$ is to perform the unitary operator U_i on the target system $\mathcal{H}_m^2$ when the state of $\mathcal{H}_n^1$ is $|i\rangle_1$. The quantum circuit representation of such a gate is shown in figure 1(d). Equivalently, the uniformly controlled unitary gate with control system $\mathcal{H}_m^2$ is defined in the same manner as described above. For example, given a real diagonal matrix $D_m = \sum_{k=1}^{m} \theta_k |k\rangle\langle k|$, we find that

$$\begin{aligned} \exp\left(-\mathrm{i}\sigma_{\varphi_n}^{ij} \otimes D_m\right) &= \exp\left(-\sum_{k=1}^{m} \theta_k \mathrm{i}\sigma_{\varphi_n}^{ij} \otimes |k\rangle\langle k|\right) \\ &= \sum_{k=1}^{m} \exp\left(-\theta_k \mathrm{i}\sigma_{\varphi_n}^{ij} \otimes |k\rangle\langle k|\right) \\ &= \sum_{k=1}^{m} \exp\left(-\theta_k \mathrm{i}\sigma_{\varphi_n}^{ij}\right) \otimes |k\rangle\langle k| \\ &= \sum_{k=1}^{m} R_{\varphi_n}^{ij}(2\theta_k) \otimes |k\rangle\langle k|. \end{aligned} \tag{11}$$

The second equality follows from the commutativity of $\sigma_{\varphi_n}^{ij} \otimes |k\rangle\langle k|$ and $\sigma_{\varphi_n}^{ij} \otimes |l\rangle\langle l|$ when $k \neq l$, and the last equality is due to equation (2). Hence, $\exp(-\mathrm{i}\sigma_{\varphi_n}^{ij} \otimes D_m)$ is a uniformly controlled $R_{\varphi_n}^{ij}$ gate with the control system $\mathcal{H}_m^2$. In the subsequent discussion, we denote $R_{\varphi_n}^{ij}$ simply as R_{φ_n} if the indices ij are unimportant in the context.

3. Quantum circuits for quNit–quMit controlled unitary operations

3.1. Quantum circuits for controlled unitary gates

Brennen *et al* [42] uses $2n$ $\mathrm{C}_k(X_m)$ gates to implement $\mathrm{C}_k(U)$. Now we use local operations and only two $\mathrm{C}_k(X_m)$ gates to implement $\mathrm{C}_k(U)$. Since the unitary matrix is diagonalizable, it may be assumed that $U = W \cdot \exp(\mathrm{i}D_m) \cdot W^\dagger$, where W is a unitary matrix and $D_m = \sum_{k=1}^{m} \theta_k |k\rangle\langle k|$ is a real diagonal matrix. From equation (7), $\mathrm{C}_k(U)$ is equivalent to a controlled diagonal gate

$$\begin{aligned} \mathrm{C}_k\left(e^{\mathrm{i}D_m}\right) &= \exp\left(|k\rangle\langle k| \otimes \mathrm{i}D_m\right) \\ &= |k\rangle\langle k| \otimes \exp\left(\mathrm{i}D_m\right) + \sum_{i=1, i\neq k}^{n} |i\rangle\langle i| \otimes I_m, \end{aligned} \tag{12}$$

up to two local operations, as shown in figure 2(a). It therefore suffices to focus on the decomposition of $\mathrm{C}_k(e^{\mathrm{i}D_m})$.

We first express $D_m = \mathrm{diag}\{\theta_1, \ldots, \theta_m\}$ as a linear combination of a set of special diagonal matrices. Let diagonal matrices $E_1 = I_m$, and for $i \in \{2, \ldots, m\}$,

$$\begin{aligned} E_i &= \sigma_{z_m}^{i-1,i} - X_m \cdot \sigma_{z_m}^{i-1,i} \cdot X_m^\dagger \\ &= \begin{cases} \sigma_{z_m}^{i-1,i} - \sigma_{z_m}^{i,i+1}, & \text{if } i \in \{2, \ldots, m-1\}, \\ \sigma_{z_m}^{m-1,m} + \sigma_{z_m}^{1,m}, & \text{if } i = m. \end{cases} \end{aligned} \tag{13}$$

Since the set $\{I_m, \sigma_{z_m}^{1,2}, \ldots, \sigma_{z_m}^{m-1,m}\}$ is linearly independent and $\sigma_{z_m}^{1,m} = \sum_{i=2}^{m} \sigma_{z_m}^{i-1,i}$, one can easily deduce that $\{E_1, \ldots, E_m\}$ is also linearly independent by the fact that

$$\sigma_{z_m}^{i-1,i} = \sum_{k=i}^{m} E_k - \sigma_{z_m}^{1,m}, \quad \sigma_{z_m}^{1,m} = \frac{\sum_{l=2}^{m} (l-1) E_l}{m}. \tag{14}$$

Hence, there exist unique real numbers $x_1, \ldots, x_m$ such that $D_m = \sum_{i=1}^{m} x_i E_i$. Furthermore, one has that

$$\begin{aligned}
\exp(\mathrm{i} D_m) &= \prod_{i=1}^{m} \exp(\mathrm{i} x_i E_i) \\
&= e^{\mathrm{i} x_1} \prod_{i=2}^{m} \exp\left[\mathrm{i} x_i \left(\sigma_{z_m}^{i-1,i} - X_m \cdot \sigma_{z_m}^{i-1,i} \cdot X_m^{\dagger}\right)\right] \\
&= e^{\mathrm{i} x_1} \prod_{i=2}^{m} \left[\exp\left(\mathrm{i} x_i \sigma_{z_m}^{i-1,i}\right) \cdot \exp\left(-\mathrm{i} x_i X_m \cdot \sigma_{z_m}^{i-1,i} \cdot X_m^{\dagger}\right)\right] \\
&= e^{\mathrm{i} x_1} \prod_{i=2}^{m} \exp\left(\mathrm{i} x_i \sigma_{z_m}^{i-1,i}\right) \cdot \prod_{i=2}^{m} \exp\left(-\mathrm{i} x_i X_m \cdot \sigma_{z_m}^{i-1,i} \cdot X_m^{\dagger}\right) \\
&= e^{\mathrm{i} x_1} \prod_{i=2}^{m} R_{z_m}^{i-1,i}(-2x_i) \cdot X_m \cdot \prod_{i=2}^{m} R_{z_m}^{i-1,i}(2x_i) \cdot X_m^{\dagger}.
\end{aligned} \tag{15}$$

In the derivation of equation (15), the second equality follows from equation (13); the third and fourth equalities follow the fact that $X_m \cdot \sigma_{z_m}^{i-1,i} \cdot X_m^{\dagger}$ is a diagonal matrix; in the last equality we use equation (2) and the relation $\exp(B \cdot A \cdot B^{-1}) = B \cdot \exp(A) \cdot B^{-1}$, where B^{-1} denotes the inverse matrix of B. Let $R_z^{\pm} = \prod_{i=2}^{m} R_{z_m}^{i-1,i}(\pm 2x_i)$. From equations (15) and (7), we have

$$\mathrm{C}_k\left(e^{\mathrm{i} D_m}\right) = \mathrm{C}_k\left(e^{\mathrm{i} x_1} I_m\right) \cdot \mathrm{C}_k\left(R_z^{-} \cdot X_m \cdot R_z^{+}\right) \cdot \mathrm{C}_k\left(X_m^{\dagger}\right). \tag{16}$$

By the definition of $R_{z_m}^{ij}(\theta)$, it follows that $(R_{z_m}^{ij}(\theta))^{\dagger} = R_{z_m}^{ij}(-\theta)$. Then, one has that

$$\left(R_z^{+}\right)^{\dagger} = R_z^{-}. \tag{17}$$

In addition, the first term $\mathrm{C}_k(e^{\mathrm{i} x_1} I_m)$ in the left-hand side of equation (16) is essentially a local diagonal operator on $\mathcal{H}_n^1$ through the following equation

$$\begin{aligned}
\mathrm{C}_k\left(e^{\mathrm{i} x_1} I_m\right) &= |k\rangle\langle k| \otimes e^{\mathrm{i} x_1} I_m + \sum_{i=1, i\neq k}^{n} |i\rangle\langle i| \otimes I_m \\
&= \exp(\mathrm{i} D) \otimes I_m.
\end{aligned} \tag{18}$$

Here the diagonal matrix $D = x_1 |k\rangle\langle k|$. From equations (17), (7), and (18), we obtain

$$\mathrm{C}_k\left(e^{\mathrm{i} D_m}\right) = \exp(\mathrm{i} D) \otimes R_z^{-} \cdot \mathrm{C}_k(X_m) \cdot I_n \otimes R_z^{+} \cdot \mathrm{C}_k\left(X_m^{\dagger}\right). \tag{19}$$

Figure 2(b) shows an equivalent quantum circuit of $\mathrm{C}_k(e^{\mathrm{i} D_m})$ based on equation (19). Here $\mathrm{C}_k(X_m^{\dagger})$ can be implemented by $\mathrm{C}_k(X_m)$ and local operations from figure 1(c). Hence, combining with figure 2(a), local operations and two $\mathrm{C}_k(X_m)$ are sufficient to implement $\mathrm{C}_k(U)$.

3.2. Quantum circuits for uniformly controlled unitary gates

Applying the above results, we can obtain a decomposition of the uniformly controlled unitary gate $\sum_{i=1}^{n} |i\rangle\langle i| \otimes U_i$ with the control system $\mathcal{H}_n^1$. For every $k \in \{1, \ldots, n\}$, we have

$$\begin{aligned}
\sum_{i=1}^{n} |i\rangle\langle i| \otimes U_i &= \prod_{i=1}^{n} \mathrm{C}_i(U_i) \\
&= I_n \otimes U_k \cdot I_n \otimes U_k^{\dagger} \cdot \prod_{i=1}^{n} \mathrm{C}_i(U_i) \\
&= I_n \otimes U_k \cdot \prod_{i=1}^{n} \mathrm{C}_i\left(U_k^{\dagger}\right) \cdot \prod_{i=1}^{n} \mathrm{C}_i(U_i) \\
&= I_n \otimes U_k \cdot \prod_{i=1, i\neq k}^{n} \mathrm{C}_i\left(U_k^{\dagger} U_i\right),
\end{aligned} \tag{20}$$

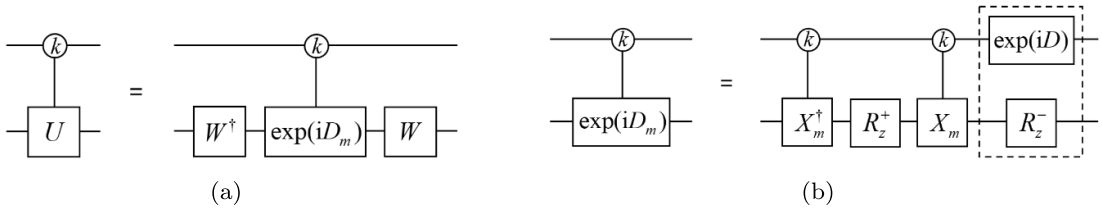

Figure 2. (a) Equivalent quantum circuit for $\mathrm{C}_k(U)$ composed of a controlled diagonal gate and two local operations. (b) Equivalent quantum circuit for $\mathrm{C}_k(e^{iD_m})$ based on equation (19). Since $\mathrm{C}_k(X_m)\cdot I_n\otimes R_z^+\cdot \mathrm{C}_k(X_m^\dagger)$ in equation (19) is a diagonal matrix, the local operations in the dotted box can be moved to the left of $\mathrm{C}_k(X_m^\dagger)$.

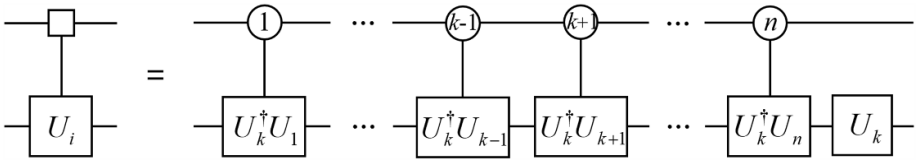

Figure 3. Equivalent quantum circuit for the uniformly controlled unitary gate $\sum_{i=1}^{n}|i\rangle\langle i|\otimes U_i$. Here $k\in\{1,\ldots,n\}$. From equation (7), the order of the $n-1$ controlled unitary gates can be arranged arbitrarily.

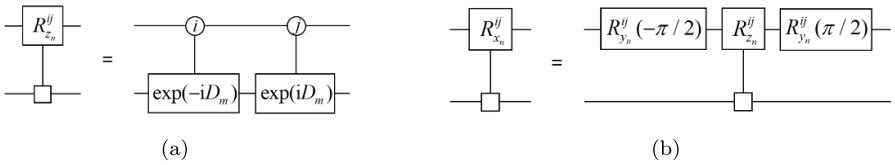

Figure 4. (a) Equivalent quantum circuit for the uniformly controlled $R_{z_n}^{ij}$ gate with control system $\mathcal{H}_m^2$. (b) Equivalent quantum circuit for the uniformly controlled $R_{x_n}^{ij}$ gate with control system $\mathcal{H}_m^2$.

where the last equality follows from the third and fourth formulas in equation (7). Hence, $\sum_{i=1}^{n}|i\rangle\langle i|\otimes U_i$ is equivalent to $(n-1)$ control unitary gates $\{\mathrm{C}_i(U_k^\dagger U_i)|1\leqslant i\leqslant n,\ i\neq k\}$ under the action of one local operation, as shown in figure 3. Together with figure 2, it is clear that a uniformly controlled unitary gate with control system $\mathcal{H}_n^1$ can be implemented by local gates and $2(n-1)$ controlled-X_m gates.

Moreover, from equation (11), it is known that $\exp(-\mathrm{i}\sigma_{z_n}^{ij}\otimes D_m)$ is a uniformly controlled $R_{z_n}^{ij}$ gate with control system $\mathcal{H}_m^2$, where $D_m=\sum_{k=1}^{m}\theta_k|k\rangle\langle k|$. By the definition of $\sigma_{z_n}^{ij}$, we have

$$\begin{aligned}\exp\left(-\mathrm{i}\sigma_{z_n}^{ij}\otimes D_m\right)&=\exp\left[\mathrm{i}\left(|j\rangle\langle j|-|i\rangle\langle i|\right)\otimes D_m\right]\\&=\exp\left(|j\rangle\langle j|\otimes \mathrm{i}D_m\right)\cdot\exp\left[|i\rangle\langle i|\otimes(-\mathrm{i}D_m)\right]\\&=\mathrm{C}_j\left(e^{\mathrm{i}D_m}\right)\cdot\mathrm{C}_i\left(e^{-\mathrm{i}D_m}\right).\end{aligned}\tag{21}$$

Thus, such an operator can be decomposed into a product of two controlled diagonal gates $\mathrm{C}_i(e^{-\mathrm{i}D_m})$ and $\mathrm{C}_j(e^{\mathrm{i}D_m})$, as shown in figure 4(a). Moreover, we find

$$\sigma_{x_n}^{ij}=R_{y_n}^{ij}\left(\frac{\pi}{2}\right)\cdot\sigma_{z_n}^{ij}\cdot R_{y_n}^{ij}\left(-\frac{\pi}{2}\right).\tag{22}$$

Together with $(R_{y_n}^{ij}(\frac{\pi}{2}))^\dagger=R_{y_n}^{ij}(-\frac{\pi}{2})$, we have

$$\exp\left(-\mathrm{i}\sigma_{x_n}^{ij}\otimes D_m\right)=R_{y_n}^{ij}\left(\frac{\pi}{2}\right)\otimes I_m\cdot\exp\left(-\mathrm{i}\sigma_{z_n}^{ij}\otimes D_m\right)\cdot R_{y_n}^{ij}\left(-\frac{\pi}{2}\right)\otimes I_m.\tag{23}$$

Based on equation (23), one finds that a uniformly controlled $R_{x_n}^{ij}$ gate is equivalent to a uniformly controlled $R_{z_n}^{ij}$ gate up to local $R_{y_n}^{ij}$ gates, as shown in figure 4(b). From figure 2(b), 4 controlled-X_m gates are sufficient to implement a uniformly controlled $R_{z_n}^{ij}$ ($R_{x_n}^{ij}$) gate with control system $\mathcal{H}_m^2$. In addition, when $n=3$, only 3 controlled-X_m gates are sufficient, by applying figure 1(a) in [43].

4. Quantum circuits for general quNit–quMit gates

Next, we show that $\mathrm{C}_n(X_m)$ and local gates form a universal set for HD quantum computation. The CSD provides an effective technique for synthesizing arbitrary multi-qubit quantum gates [49] as well as general HD quantum gates [45]. In the following, we use CSD to give a recursive decomposition that breaks down general unitary operations on $\mathcal{H}_n^1 \otimes \mathcal{H}_m^2$ into a product of uniformly controlled unitary gates with the control system $\mathcal{H}_n^1$ and uniformly controlled R_{x_n} gates with the control system $\mathcal{H}_m^2$.

4.1. Synthesis algorithm of general quNit–quMit gates

Let $U(n)$ denote the unitary group of $n \times n$ unitary matrices. A general unitary operation on $\mathcal{H}_n^1 \otimes \mathcal{H}_m^2$ can be recognized as an element of $U(nm)$.

Cosine–sine decomposition (CSD).—Let $X \in U(nm)$ be a unitary matrix partitioned as

$$X = \begin{bmatrix} X_{11} & X_{12} \\ X_{21} & X_{22} \end{bmatrix}, \tag{24}$$

where X_{11} is a $\lfloor \frac{n}{2} \rfloor m \times \lfloor \frac{n}{2} \rfloor m$ matrix and X_{22} is a $(n - \lfloor \frac{n}{2} \rfloor)m \times (n - \lfloor \frac{n}{2} \rfloor)m$ matrix. For convenience, setting $n_1 = \lfloor \frac{n}{2} \rfloor$ and $n_2 = n - \lfloor \frac{n}{2} \rfloor$, we have $0 < n_1 \leqslant n_2 < n$ and $n_1 + n_2 = n$. The CSD [44, 45, 53] factorizes X into a product of three matrices:

$$X = \begin{bmatrix} U_1 & \mathbf{0} \\ \mathbf{0} & \bar{U}_2 \end{bmatrix} \cdot \begin{bmatrix} C & -S & \mathbf{0} \\ S & C & \mathbf{0} \\ \mathbf{0} & \mathbf{0} & I_{(n_2-n_1)m} \end{bmatrix} \cdot \begin{bmatrix} U_1' & \mathbf{0} \\ \mathbf{0} & \bar{U}_2' \end{bmatrix}, \tag{25}$$

where $U_1, U_1' \in U(n_1 m)$, $\bar{U}_2, \bar{U}_2' \in U(n_2 m)$, and C, S are $n_1 m \times n_1 m$ real diagonal matrices satisfying $C^2 + S^2 = I_{n_1}$.

In [45], the second matrix in the right-hand side of equation (25) can be expressed as a product of uniformly controlled R_{y_n} gates with the control system $\mathcal{H}_m^2$. Next, we make a slight modification to equation (25) such that the second matrix becomes a product of uniformly controlled R_{x_n} gates with the control system $\mathcal{H}_m^2$.

The first decomposition of $U(nm)$.—From equation (25), we can get a decomposition of $X \in U(nm)$ as

$$X = U \cdot V \cdot U' \tag{26}$$

where

$$V = \begin{bmatrix} C & -\mathrm{i}S & \mathbf{0} \\ -\mathrm{i}S & C & \mathbf{0} \\ \mathbf{0} & \mathbf{0} & I_{(n_2-n_1)m} \end{bmatrix}. \tag{27}$$

$$\begin{aligned} U &= \begin{bmatrix} U_1 & \mathbf{0} \\ \mathbf{0} & U_2 \end{bmatrix}, \; U_2 = \bar{U}_2 \cdot \begin{bmatrix} \mathrm{i}I_{n_1 m} & \mathbf{0} \\ \mathbf{0} & I_{(n_2-n_1)m} \end{bmatrix}, \\ U' &= \begin{bmatrix} U_1' & \mathbf{0} \\ \mathbf{0} & U_2' \end{bmatrix}, \; U_2' = \begin{bmatrix} -\mathrm{i}I_{n_1 m} & \mathbf{0} \\ \mathbf{0} & I_{(n_2-n_1)m} \end{bmatrix} \cdot \bar{U}_2'. \end{aligned} \tag{28}$$

We now explain that V can be expressed as a product of uniformly controlled R_{x_n} gates. Without loss of generality, we may assume

$$\begin{aligned} C &= \mathrm{diag}\{\cos\theta_{11}, \ldots, \cos\theta_{1m}, \cos\theta_{21}, \ldots, \cos\theta_{n_1 m}\}, \\ S &= \mathrm{diag}\{\sin\theta_{11}, \ldots, \sin\theta_{1m}, \sin\theta_{21}, \ldots, \sin\theta_{n_1 m}\}. \end{aligned} \tag{29}$$

One can verify that

$$V = \exp\left\{\sum_{i=1}^{n_1} -\mathrm{i}\sigma_{x_n}^{i,n_1+i} \otimes D_m^{(i)}\right\} = \prod_{i=1}^{n_1} \exp\left(-\mathrm{i}\sigma_{x_n}^{i,n_1+i} \otimes D_m^{(i)}\right), \tag{30}$$

where the first equality is obtained by letting the diagonal matrix $D_m^{(i)} = \mathrm{diag}\{\theta_{i1}, \ldots, \theta_{im}\}$; the second equality follows from the commutativity of two matrices $\sigma_{x_n}^{i,n_1+i}$ and $\sigma_{x_n}^{j,n_1+j}$.

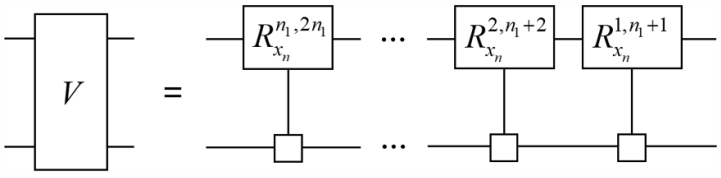

Figure 5. Quantum circuit for the non-local operation V given by equation (30). Here $n_1 = \lfloor \frac{n}{2} \rfloor$.

From equations (11) and (30), V is equivalent to $\lfloor \frac{n}{2} \rfloor$ uniformly controlled R_{x_n} gates with the control system $\mathcal{H}_m^2$, as shown in figure 5. Hence, combining with figures 2(b) and 4, local operations and $4\lfloor \frac{n}{2} \rfloor$ controlled-X_m gates are sufficient to implement V exactly.

From equations (25) and (28), $U_1, U_1' \in U(n_1 m)$ and $U_2, U_2' \in U(n_2 m)$. If $n_1 = n_2 = 1$ (i.e. $n = 2$), U and U' are uniformly controlled unitary gates with the control system $\mathcal{H}_2^1$, which can be synthesized by figures 3 and 2. In this case, the synthesis of X is completed. Otherwise, one can find that $U, U' \in U(n_1 m) \oplus U(n_2 m)$ can be further decomposed using equation (26) as follows.

The second decomposition of $U(nm)$.— Here we take U as an example, and U' will follow a similar discussion to U. We first discuss the case where $n_1 > 1$. Applying equation (26) to decompose U_1 and U_2, we get

$$\begin{bmatrix} U_1 & \mathbf{0} \\ \mathbf{0} & U_2 \end{bmatrix} = \begin{bmatrix} W_1 & \mathbf{0} \\ \mathbf{0} & W_2 \end{bmatrix} \cdot \begin{bmatrix} V_1 & \mathbf{0} \\ \mathbf{0} & V_2 \end{bmatrix} \cdot \begin{bmatrix} W_1' & \mathbf{0} \\ \mathbf{0} & W_2' \end{bmatrix}. \tag{31}$$

From equation (30), V_1 and V_2 in equation (31) can be expressed as

$$V_k = \prod_{i=1}^{\lfloor \frac{n_k}{2} \rfloor} \exp\left(-\mathrm{i}\sigma_{x_{n_k}}^{i,\lfloor \frac{n_k}{2} \rfloor + i} \otimes D_m^{(k,i)}\right), \quad k \in \{1,2\}, \tag{32}$$

where $D_m^{(k,i)}$ is a real diagonal matrix. One can simply verify that

$$\begin{aligned} \begin{bmatrix} V_1 & \mathbf{0} \\ \mathbf{0} & V_2 \end{bmatrix} &= \begin{bmatrix} V_1 & \mathbf{0} \\ \mathbf{0} & I_{n_2} \end{bmatrix} \cdot \begin{bmatrix} I_{n_1} & \mathbf{0} \\ \mathbf{0} & V_2 \end{bmatrix}, \\ \begin{bmatrix} V_1 & \mathbf{0} \\ \mathbf{0} & I_{n_2} \end{bmatrix} &= \prod_{i=1}^{\lfloor \frac{n_1}{2} \rfloor} \exp\left(-\mathrm{i}\sigma_{x_n}^{i,\lfloor \frac{n_1}{2} \rfloor + i} \otimes D_m^{(1,i)}\right), \\ \begin{bmatrix} I_{n_1} & \mathbf{0} \\ \mathbf{0} & V_2 \end{bmatrix} &= \prod_{i=1}^{\lfloor \frac{n_2}{2} \rfloor} \exp\left(-\mathrm{i}\sigma_{x_n}^{n_1+i,n_1+\lfloor \frac{n_2}{2} \rfloor + i} \otimes D_m^{(2,i)}\right). \end{aligned} \tag{33}$$

From equation (33), the non-local operation $V_1 \oplus V_2$ in equation (31) is equivalent to $\lfloor \frac{n_1}{2} \rfloor + \lfloor \frac{n_2}{2} \rfloor$ uniformly controlled R_{x_n} gates with the control system $\mathcal{H}_m^2$. Hence, it can be implemented by local operations and $4(\lfloor \frac{n_1}{2} \rfloor + \lfloor \frac{n_2}{2} \rfloor)$ controlled-X_m gates from figures 2(b) and 4.

As for $W_1 \oplus W_2$ (and similarly for $W_1' \oplus W_2'$) in equation (31), from equations (26) and (28), we have

$$\begin{bmatrix} W_1 & \mathbf{0} \\ \mathbf{0} & W_2 \end{bmatrix} = \begin{bmatrix} W_{11} & \mathbf{0} & \mathbf{0} & \mathbf{0} \\ \mathbf{0} & W_{12} & \mathbf{0} & \mathbf{0} \\ \mathbf{0} & \mathbf{0} & W_{21} & \mathbf{0} \\ \mathbf{0} & \mathbf{0} & \mathbf{0} & W_{22} \end{bmatrix}, \tag{34}$$

where $W_{11} \in U(\lfloor \frac{n_1}{2} \rfloor m)$, $W_{12} \in U((n_1 - \lfloor \frac{n_1}{2} \rfloor)m)$, $W_{21} \in U(\lfloor \frac{n_2}{2} \rfloor m)$, and $W_{22} \in U((n_2 - \lfloor \frac{n_2}{2} \rfloor)m)$.

If $n_1 = 1$ and $n_2 > 1$ (i.e. $n_2 = 2$), it is only necessary to decompose U_2, in which $W_1 = U_1$ and $W_1' = V_1 = I_m$ in equation (31). For this case, since $U_1, W_{21}, W_{22} \in U(m)$,

$$\begin{bmatrix} W_1 & \mathbf{0} \\ \mathbf{0} & W_2 \end{bmatrix} = \begin{bmatrix} U_1 & \mathbf{0} & \mathbf{0} \\ \mathbf{0} & W_{21} & \mathbf{0} \\ \mathbf{0} & \mathbf{0} & W_{22} \end{bmatrix} \tag{35}$$

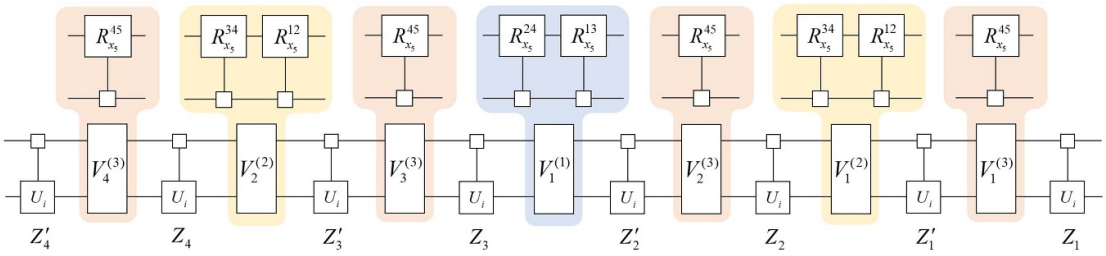

Figure 6. Quantum circuit for general unitary operations on $\mathcal{H}_5^1 \otimes \mathcal{H}_m^2$. Appendix A provides a detailed explanation.

is a uniformly controlled unitary gate and its implementation is shown in figures 3 and 2. Thus, in this case, the synthesis of X is completed.

Recursive decomposition of $U(nm)$.— If equation (34) is not a uniformly controlled unitary gate, the matrix in the right-hand side of equation (34) can be further decomposed following a similar argument as described above. The decomposition terminates when all block matrices W_{11}, W_{12}, W_{21}, and W_{22} reduce to a $m \times m$ matrix (i.e. equation (34) is a uniformly controlled unitary gate with control system $\mathcal{H}_n^1$). Generally, the complete process requires $d = \lceil \log_2 n \rceil$ steps of decomposition:

$$\begin{aligned} U(nm) &\xrightarrow{1} U\left(\lfloor \tfrac{n}{2} \rfloor m\right) \oplus U\left(\left(n - \lfloor \frac{n}{2} \rfloor\right) m\right) \\ &\xrightarrow{2} \left[U\left(\lfloor \tfrac{n_1}{2} \rfloor m\right) \oplus U\left(\left(n_1 - \lfloor \frac{n_1}{2} \rfloor\right) m\right)\right] \oplus \left[U\left(\lfloor \tfrac{n_2}{2} \rfloor m\right) \oplus U\left(\left(n_2 - \lfloor \frac{n_2}{2} \rfloor\right) m\right)\right] \\ &\quad \cdots \\ &\xrightarrow{d} \bigoplus_m U(n), \end{aligned} \tag{36}$$

where $n_1 = \lfloor \frac{n}{2} \rfloor$, $n_2 = n - \lfloor \frac{n}{2} \rfloor$, and $\bigoplus_m U(n)$ denotes the direct sum of m copies of $U(n)$.

Example.— When $n = 5$, for any $X \in U(5m)$, its quantum circuit obtained after 3 steps of decomposition is shown in figure 6. This process is given in appendix B.

As shown in figure 6, we write $V^{(k)}$ to denote the non-local operation in the form of the product of uniformly controlled R_{x_n} gates with the control system $\mathcal{H}_m^2$ obtained by the kth decomposition. In general, the final quantum circuit of $X \in U(nm)$ consists of 2^d uniformly controlled unitary gates with the control system $\mathcal{H}_n^1$ and $2^d - 1$ non-local operations $\{V^{(1)}, \ldots, V^{(d)}\}$. Finally, together with figures 2–4 and figure 1(c), X can be synthesized by controlled-X_m gates $\mathrm{C}_n(X_m)$ and local operations.

4.2. Further simplification of quantum circuits for general quNit–quMit gates

Note that the constructed quantum circuit of $X \in U(nm)$ is implemented by an arrangement of $ZVZV \ldots ZVZ$, where Z denotes a uniformly controlled unitary gate and V denotes the product of uniformly controlled R_{x_n} gates in the circuit. An example is shown in figure 6. From figure 3, we know that Z consists of $n-1$ controlled unitary gates. Applying the commutativity of matrices, we can further reduce the number of controlled unitary gates generated by the implementation of Z.

In particular, when n is odd, it follows from equations (27) and (30) that

$$V = \begin{bmatrix} \widetilde{V} & \mathbf{0} \\ \mathbf{0} & I_m \end{bmatrix} = \prod_{i=1}^{\frac{n-1}{2}} \exp\left(-\mathrm{i}\sigma_{x_n}^{i,\frac{n-1}{2}+i} \otimes D_m^{(i)}\right), \tag{37}$$

where $\widetilde{V}$ is a certain $(n-1)m \times (n-1)m$ unitary matrix. Indeed, it can be calculated that

$$\widetilde{V} = \begin{bmatrix} C & -\mathrm{i}S \\ -\mathrm{i}S & C \end{bmatrix} = \prod_{i=1}^{\frac{n-1}{2}} \exp\left(-\mathrm{i}\sigma_{x_{n-1}}^{i,\frac{n-1}{2}+i} \otimes D_m^{(i)}\right). \tag{38}$$

Hence, from equation (6), it holds that

$$\mathrm{C}_n(U) \cdot V = V \cdot \mathrm{C}_n(U), \tag{39}$$

where U is a unitary operator on $\mathcal{H}_m^2$. From equation (39), $\mathrm{C}_n(U)$ generated by Z can be transferred to the right side of V, and then combined with Z' in the next block to form a new uniformly controlled

unitary gate. Thus, we can eliminate one controlled unitary gate, which reduces two controlled-X_m gates in the circuit.

Here we still assume $n=5$ to explain how to eliminate some controlled unitary gates in figure 6. From equations (49), (52), and (57), it follows that

$$V^{(i)}=\begin{bmatrix}\widetilde{V}^{(i)} & \mathbf{0}\\ \mathbf{0} & I_m\end{bmatrix},\ V^{(3)}=\begin{bmatrix}I_{3m} & \mathbf{0}\\ \mathbf{0} & \widetilde{V}^{(3)}\end{bmatrix}, \tag{40}$$

where $i\in\{1,2\}$ and

$$\begin{aligned}\widetilde{V}^{(1)}&=\exp\left(-\mathrm{i}\sigma_{x_4}^{13}\otimes D_m^{(1)}\right)\cdot\exp\left(-\mathrm{i}\sigma_{x_4}^{24}\otimes D_m^{(2)}\right),\\ \widetilde{V}^{(2)}&=\exp\left(-\mathrm{i}\sigma_{x_4}^{12}\otimes D_m^{(3)}\right)\cdot\exp\left(-\mathrm{i}\sigma_{x_4}^{34}\otimes D_m^{(4)}\right),\\ \widetilde{V}^{(3)}&=\exp\left(-\mathrm{i}\sigma_{x_2}^{12}\otimes D_m^{(5)}\right).\end{aligned} \tag{41}$$

Thus, it holds that

$$\begin{aligned}&\mathrm{C}_5(U)\cdot V^{(i)}=V^{(i)}\cdot\mathrm{C}_5(U),\ \ i\in\{1,2\},\\ &\mathrm{C}_j(U)\cdot V^{(3)}=V^{(3)}\cdot\mathrm{C}_j(U),\ \ j\in\{1,2,3\}.\end{aligned} \tag{42}$$

In figure 6, equation (42) implies that $\mathrm{C}_5(U)$ (resp. $\mathrm{C}_j(U)$), which arises from the synthesis of Z_k ($k\in\{2,3,4\}$) (resp. Z_l' ($l\in\{1,2,3,4\}$)) on the left of $V^{(i)}$ (resp. $V^{(3)}$), can be absorbed by Z_{k-1}' (resp. Z_l) on the right of $V^{(i)}$ (resp. $V^{(3)}$). Thus, for the implementation of Z_k ($k\in\{2,3,4\}$), we can omit one controlled unitary gate; Z_l' ($l\in\{1,2,3,4\}$) can omit three controlled unitary gates. Therefore, 15 controlled unitary gates in figure 6 may be omitted.

5. Quantum gate count

Below, we calculate the number of controlled-X_m gates required to synthesize a general unitary operation $X\in U(nm)$ on $\mathcal{H}_n^1\otimes\mathcal{H}_m^2$ by this scheme. For this purpose, it is only sufficient to identify the number of uniformly controlled R_{x_n} gates with the control system $\mathcal{H}_m^2$ required for the synthesis of $V^{(k)}$, where $k\in\{1,\ldots,d\}$, and the number of controlled unitary gates that can be eliminated.

Given a positive integer n, let $d=\lceil\log_2 n\rceil$ and $n(1,1)=n$. Fix an integer $k\in\{2,\ldots,d\}$. For $i\in\{1,\ldots,2^{k-1}\}$, we define

$$n(k,i)=\begin{cases}\lfloor n\left(k-1,\frac{i+1}{2}\right)\rfloor, & \text{if } i \text{ is odd},\\ n\left(k-1,\frac{i}{2}\right)-\lfloor n\left(k-1,\frac{i}{2}\right)\rfloor, & \text{if } i \text{ is even}.\end{cases} \tag{43}$$

Then we get the decomposition $n=\sum_{i=1}^{2^{k-1}}n(k,i)$ for each $k\in\{1,2,\ldots,d\}$. For example,

$$\begin{aligned}5&=2+3\\ &=(1+1)+(1+2),\end{aligned} \tag{44}$$

where one has $5(1,1)=5$, $5(2,1)=2$, $5(2,2)=3$, $5(3,1)=5(3,2)=5(3,3)=1$, and $5(3,4)=2$.

For $k\in\{1,\ldots,d\}$, let $N_n^{(k)}$ denote the number of odd integers in the set $\{n(k,1),\ldots,n(k,2^{k-1})\}$, i.e.

$$N_n^{(k)}=\sum_{i=1}^{2^{k-1}}[n(k,i)\bmod 2]. \tag{45}$$

From the decomposition given in equation (26), $N_n^{(k)}$ means the number of identity matrices I_m in the diagonal blocks of $V^{(k)}$. For the case $n=5$, we have $N_5^{(1)}=N_5^{(2)}=1$ and $N_5^{(3)}=3$. Comparing with equation (40), it can be observed that $N_5^{(1)}$, $N_5^{(2)}$, and $N_5^{(3)}$ indeed correspond to the number of the identity matrices I_m in the diagonal blocks of $V^{(1)}$, $V^{(2)}$, and $V^{(3)}$, respectively.

Based on the method described in section 4.2, the number of controlled unitary gates that can be eliminated is equal to the number of identity matrices I_m in the diagonal blocks of $V^{(k)}$. Therefore, the number of controlled unitary gates that can be eliminated is $\sum_{k=1}^{d}2^{k-1}N_n^{(k)}$ by the fact that there are

Table 1. Comparison of the number of imprimitive gates required to synthesize a general unitary operation on $\mathcal{H}_n^1 \otimes \mathcal{H}_n^2$ by several schemes.

Synthesis	Imprimitive	Gate count for $3 \leqslant n \leqslant 8$					
algorithm	gates	3	4	5	6	7	8
QSD [44]	GCX	26	90	176	355	618	980
QSD [38]	CDNOT	—	60	—	—	—	—
QR [42]	CINC & CINC^{-1}	78	220	495	996	1708	2808
CSD [45]	CINC & CINC^{-1}	36	72	280	420	588	784
Our	CINC	**19**	**48**	**74**	**116**	**166**	**224**

2^{k-1} non-local operations $V^{(k)}$ in the quantum circuit of X. Moreover, the quantum circuit of $V^{(k)}$ consists of $\frac{n-N_n^{(k)}}{2}$ uniformly controlled R_{x_n} gates with the control system $\mathcal{H}_m^2$.

There are 2^d uniformly controlled unitary gates with the control system $\mathcal{H}_n^1$ in the quantum circuit of X. Thus, the number of controlled-X_m gates required to synthesize a general quNit–quMit gate X is at most

$$(2n-1)\,2^{\lceil \log_2 n\rceil+1} - 2n - \sum_{k=1}^{\lceil \log_2 n\rceil} 2^{k+1} N_n^{(k)}. \tag{46}$$

Since $2^{\lceil \log_2 n\rceil+1} = O(n)$, the quantum circuit of $X \in U(nm)$ is implemented by $O(n^2)$ controlled-X_m gates. Appendix C gives a code to calculate the number of CINC gates. Table 1 shows a comparison of the number of quantum gates with the previous synthesis schemes.

Moreover, for $\mathcal{H}_n^1 \otimes \mathcal{H}_n^2$, [54] shows that $O(n^4)$ controlled-phase gates $e^{i\pi|n\rangle\langle n|\otimes|n\rangle\langle n|}$ are required to implement a general unitary gate on $\mathcal{H}_n^1 \otimes \mathcal{H}_n^2$. From equation (16) in [54], a controlled-X_n gate can be implemented by $n-1$ controlled-phase gates. Thus, our protocol requires at most $O(n^3)$ controlled-X_n gates to implement a two-quNit gate, which establishes a better upper bound than the $O(n^4)$ complexity in [54].

6. Conclusion

We have presented a recursive algorithm to exactly synthesize an arbitrary unitary operation on $\mathcal{H}_n^1 \otimes \mathcal{H}_m^2$. The constructed quantum circuit for a general unitary operation consists of the controlled-X_m gate $\mathrm{C}_n(X_m)$ and local gates without ancillary quantum systems. The control states of all controlled-X_m gates in the quantum circuit are located on the system $\mathcal{H}_n^1$. Since an arbitrary multi-quNit gate can be exactly simulated by two-quNit gates [46], our scheme shows that $\mathrm{C}_n(X_m)$ and local gates are universal for HD quantum computation.

The number of $\mathrm{C}_n(X_m)$ in the circuit is given by equation (46), which is determined by the dimension of $\mathcal{H}_n^1$ and independent of $\mathcal{H}_m^2$. Combined with the trick of ignoring controlled unitary gates, the number of $\mathrm{C}_n(X_m)$ in the circuit is greatly reduced compared with previous works. As shown in table 1, the result shows that the complexity of our circuit is the lowest currently known. Our scheme is not limited to a particular physical system, which has potential for HD quantum computation. Future research directions include extending the quantum circuit to multi-component systems (involving more than two systems) and designing experimental schemes for this quantum circuit.

Data availability statement

All data that support the findings of this study are included within the article (and any supplementary files).

Funding

This work is supported by the National Natural Science Foundation of China under Grant No. 62371038.

Author contributions

Both authors had equal contributions to the paper.

Appendix A. Experimental implementation of CINC gates

We now present an experimental scheme to implement the controlled-X_m gate $C_n(X_m)$ following the method in [25]. Here we take $C_3(X_3)$ on $\mathcal{H}_3^1 \otimes \mathcal{H}_3^2$ as an example, while the generalization to arbitrary dimensions follows similarly (see also supplementary material of [25]). We consider the orbital angular momentum (OAM) degree of freedom of photons as the quantum states, which means that $|l\rangle$ denotes a single photon with OAM value l.

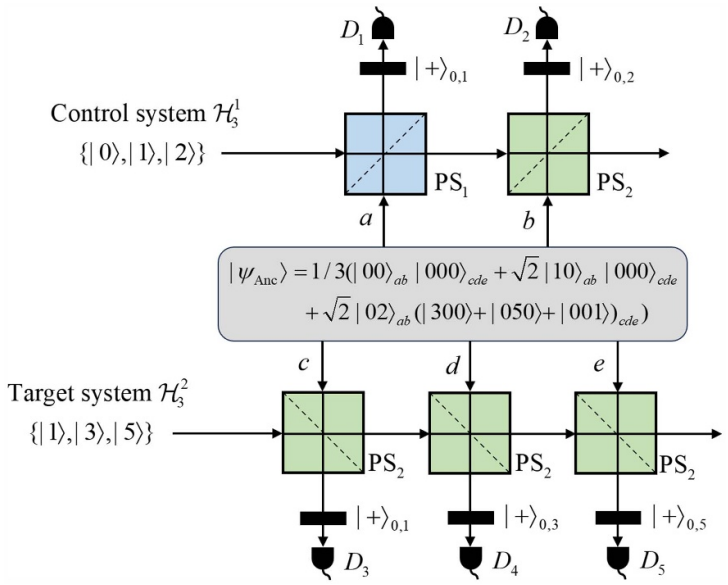

Figure 7. Experimental setup of controlled increment gates for $\mathcal{H}_3^1 \otimes \mathcal{H}_3^2$. Here PS_1 denotes a parity sorter, which transmits even modes $\{|0\rangle, |2\rangle, \ldots\}$ and reflects odd modes $\{|1\rangle, |3\rangle, \ldots\}$. PS_2 denotes a second-order parity sorter, which transmits modes $|2k \times 2\rangle$ $(k = 0, 1, 2, \ldots)$ and reflects modes $|(2k-1) \times 2\rangle$. If the input is an odd mode, then PS_2 transmits the photon with a probability of $\frac{1}{2}$ and reflects the photon with equal probability. $|+\rangle_{0,k}$ denotes a mode filter, which projects the photons into the subspace $\{|0\rangle, |k\rangle\}$. D_i denotes a detector.

The experimental setup for implementing $C_3(X_3)$ is shown in figure 7. The implementation requires an ancillary quantum state

$$|\psi_{\text{Anc}}\rangle = \frac{1}{3}|00\rangle_{ab}|000\rangle_{cde} + \frac{\sqrt{2}}{3}|10\rangle_{ab}|000\rangle_{cde} + \frac{\sqrt{2}}{3}|02\rangle_{ab}(|300\rangle + |050\rangle + |001\rangle)_{cde}. \tag{47}$$

The subscripts *abcde* here mean the photons are in the corresponding paths as shown in figure 7. The desired quantum operation is heralded by the simultaneous clicks of all detectors and relies on post-selection. The only difference between this setup and figure 2 in [25] is the ancillary quantum state.

Specifically, if the state of the control system $\mathcal{H}_3^1$ is $|2\rangle$, the two detectors D_1 and D_2 click and the output state is still $|2\rangle$, only when the photons state in the paths ab is $|02\rangle_{ab}$. In other cases, either the detectors D_1 and D_2 do not all fire, or there is no photon in the output path (see also figure 2 of [25]). Thus, if the input state is $|2\rangle$ and the detectors D_1 and D_2 click, then $|\psi_{\text{Anc}}\rangle$ will collapse into $\frac{1}{\sqrt{3}}(|300\rangle + |050\rangle + |001\rangle)_{cde}$ with a probability of $2/3$. In this case, if detectors D_3–D_5 all click, the state of the target system $\mathcal{H}_3^2$ follows the transformations: $|1\rangle \to |3\rangle, |3\rangle \to |5\rangle, |5\rangle \to |1\rangle$ with a probability of $1/(2^4 \times 3)$ (see figure 1 of [25]).

If the state of $\mathcal{H}_3^1$ is $|0\rangle$ (resp. $|1\rangle$), only $|00\rangle_{ab}$ (resp. $|10\rangle_{ab}$) can cause both detectors D_1 and D_2 to click and the output state to be $|0\rangle$ (resp. $|1\rangle$). Thus, when the input state is $|0\rangle$ or $|1\rangle$ and detectors D_1 and D_2 click, $|\psi_{\text{Anc}}\rangle$ collapses into $|000\rangle_{cde}$ with a probability of $1/9$. The state $|000\rangle_{cde}$ activates detectors D_3-D_5 while leaving the output state of the target system unchanged with a probability of $1/2^3$.

Therefore, when detectors D_1–D_5 click, the quantum gate $C_3(X_3)$ is successfully implemented. The success probability of the implementation for $C_3(X_3)$ is $1/(2^3\times 9)=1/72$, regardless of the input mode of the control system.

Appendix B. Example: decomposition of elements in $U(5m)$

Assuming that $X\in U(5m)$, we will give the decomposition of X through the method described in section 4.1.

Step 1: We use equation (26) to decompose X into

$$X=U\cdot V^{(1)}\cdot U'. \tag{48}$$

From equation (30), we have

$$V^{(1)}=\exp\left(-\mathrm{i}\sigma_{x_5}^{13}\otimes D_m^{(1)}\right)\cdot\exp\left(-\mathrm{i}\sigma_{x_5}^{24}\otimes D_m^{(2)}\right), \tag{49}$$

where $D_m^{(1)}$ and $D_m^{(2)}$ are real diagonal matrices. For U, it follows from equation (25) that

$$U=\begin{bmatrix} U_1 & \mathbf{0}\\ \mathbf{0} & U_2\end{bmatrix}, \tag{50}$$

where $U_1\in U(2m)$ and $U_2\in U(3m)$. The treatment of U' parallels that of U.

Step 2: We then use equation (26) to decompose U_1 and U_2. From equation (31), we get

$$U=W\cdot V^{(2)}\cdot W'. \tag{51}$$

By equation (33), $V^{(2)}$ can be expressed as

$$V^{(2)}=\exp\left(-\mathrm{i}\sigma_{x_5}^{12}\otimes D_m^{(3)}\right)\cdot\exp\left(-\mathrm{i}\sigma_{x_5}^{34}\otimes D_m^{(4)}\right), \tag{52}$$

where $D_m^{(3)}$ and $D_m^{(4)}$ are real diagonal matrices. Moreover, from equation (34), one has

$$W=\begin{bmatrix} W_{11} & \mathbf{0} & \mathbf{0} & \mathbf{0}\\ \mathbf{0} & W_{12} & \mathbf{0} & \mathbf{0}\\ \mathbf{0} & \mathbf{0} & W_{21} & \mathbf{0}\\ \mathbf{0} & \mathbf{0} & \mathbf{0} & W_{22}\end{bmatrix}, \tag{53}$$

where $W_{11},W_{12},W_{21}\in U(m)$ and $W_{22}\in U(2m)$. An analogous discussion holds for W'.

Step 3: Finally, we just need to decompose W_{22}. Using equation (26) for W_{22}, we get

$$W_{22}=\begin{bmatrix}\widetilde{Z}_1 & \mathbf{0}\\ \mathbf{0} & \widetilde{Z}_2\end{bmatrix}\cdot\exp\left(-\mathrm{i}\sigma_{x_2}^{12}\otimes D_m^{(5)}\right)\cdot\begin{bmatrix}\widetilde{Z}_1' & \mathbf{0}\\ \mathbf{0} & \widetilde{Z}_2'\end{bmatrix}, \tag{54}$$

where $\{\widetilde{Z}_1,\widetilde{Z}_1',\widetilde{Z}_2,\widetilde{Z}_2'\}\subset U(m)$. Substituting equation (54) into equation (53), it immediately follows that

$$W=Z\cdot V^{(3)}\cdot Z', \tag{55}$$

where

$$Z=\begin{bmatrix} W_{11} & \mathbf{0} & \mathbf{0} & \mathbf{0} & \mathbf{0}\\ \mathbf{0} & W_{12} & \mathbf{0} & \mathbf{0} & \mathbf{0}\\ \mathbf{0} & \mathbf{0} & W_{21} & \mathbf{0} & \mathbf{0}\\ \mathbf{0} & \mathbf{0} & \mathbf{0} & \widetilde{Z}_1 & \mathbf{0}\\ \mathbf{0} & \mathbf{0} & \mathbf{0} & \mathbf{0} & \widetilde{Z}_2\end{bmatrix},\quad Z'=\begin{bmatrix} I_{3m} & \mathbf{0} & \mathbf{0}\\ \mathbf{0} & \widetilde{Z}_1' & \mathbf{0}\\ \mathbf{0} & \mathbf{0} & \widetilde{Z}_2'\end{bmatrix}, \tag{56}$$

and

$$\begin{aligned} V^{(3)}&=\begin{bmatrix} I_{3m} & \mathbf{0}\\ \mathbf{0} & \exp\left(-\mathrm{i}\sigma_{x_2}^{12}\otimes D_m^{(5)}\right)\end{bmatrix}\\ &=\exp\left(-\mathrm{i}\sigma_{x_5}^{45}\otimes D_m^{(5)}\right). \end{aligned} \tag{57}$$

Note that Z and Z' are uniformly controlled unitary gates with the control system $\mathcal{H}_5^1$.

Hence, from equations (48), (51) and (55), we can obtain

$$\begin{aligned} X &= U \cdot V^{(1)} \cdot U' \\ &= W_1 \cdot V_1^{(2)} \cdot W_1' \cdot V^{(1)} \cdot W_2 \cdot V_2^{(2)} \cdot W_2' \\ &= \left(Z_1 \cdot V_1^{(3)} \cdot Z_1'\right) \cdot V_1^{(2)} \cdot \left(Z_2 \cdot V_2^{(3)} \cdot Z_2'\right) \cdot V^{(1)} \\ &\quad \cdot \left(Z_3 \cdot V_3^{(3)} \cdot Z_3'\right) \cdot V_2^{(2)} \cdot \left(Z_4 \cdot V_4^{(3)} \cdot Z_4'\right). \end{aligned} \tag{58}$$

Here Z_i and Z_i' are uniformly controlled unitary gates with the control system $\mathcal{H}_5^1$. Based on equation (58), we can get the quantum circuit of X, as shown in figure 6.

Appendix C. Algorithm for the CINC gate counts

Given an arbitrary dimension n, the Wolfram code to calculate the number of CINC required to accurately implement a general quNit–quMit gate based on our scheme is shown in figure 8.

```
In[•]:= n = Input["Dimension of the first system n="];
d = Ceiling[Log[2, n]];
nij = Table[n, {i, d}, {j, 2^(i - 1)}];
For[i = 2, i ≤ d, i++,
  For[j = 1, j ≤ 2^(i - 1), j++,
   If[OddQ[j], nij[[i, j]] = Floor[nij[[i - 1, (j+1)/2]]/2],
    nij[[i, j]] = nij[[i - 1, j/2]] - Floor[nij[[i - 1, j/2]]/2]]
  ]
 ];
S = ConstantArray[0, d];
For[i = 1, i ≤ d, i++,
  For[j = 1, j ≤ 2^(i - 1), j++,
   If[OddQ[nij[[i, j]]], S[[i]] = S[[i]] + 1, S[[i]] = S[[i]] + 0]
  ]
 ];
N1 = Sum[2^(i - 1) * (n - S[[i]])/2, {i, d}];
N2 = 2^(d);
N3 = Sum[2^(i - 1) * S[[i]], {i, d}];
Column[nij, Center]
Print["The ", d, "-tuple determined by a positive integer n=", n, " is ", S]
Print["The number of uniformly controlled R_x_n^ij gates is ", N1]
Print["The number of uniformly controlled unitary gates is ", N2]
Print["The number of absorbed controlled unitary gates is ", N3]
Print["The total number of CINC gates is ", N1 * 4 + N2 * 2 (n - 1) - N3 * 2]
```

Figure 8. Code for calculating CINC gate counts in Wolfram Mathematica.

ORCID iD

Hai-Rui Wei 0000-0001-7459-4161

References

[1] Hu X-M, Guo Y, Liu B-H, Huang Y-F, Li C-F and Guo G-C 2018 Beating the channel capacity limit for superdense coding with entangled ququarts *Sci. Adv.* **4** eaat9304

[2] Brüß D and Macchiavello C 2002 Optimal eavesdropping in cryptography with three-dimensional quantum states *Phys. Rev. Lett.* **88** 127901

[3] Cerf N J, Bourennane M, Karlsson A and Gisin N 2002 Security of quantum key distribution using d-level systems *Phys. Rev. Lett.* **88** 127902

[4] Bocharov A, Roetteler M and Svore K M 2017 Factoring with qutrits: Shor's algorithm on ternary and metaplectic quantum architectures *Phys. Rev. A* **96** 012306
[5] Lu H-H, Hu Z, Alshaykh M S, Moore A J, Wang Y, Imany P, Weiner A M and Kais S 2019 Quantum phase estimation with time-frequency qudits in a single photon *Adv. Quantum Technol.* **3** 1900074
[6] Saha A, Majumdar R, Saha D, Chakrabarti A and Sur-Kolay S 2022 Asymptotically improved circuit for a *d*-ary Grover's algorithm with advanced decomposition of the *n*-qudit Toffoli gate *Phys. Rev. A* **105** 062453
[7] Lanyon B P, Weinhold T J, Langford N K, O'Brien J L, Resch K J, Gilchrist A and White A G 2008 Manipulating biphotonic qutrits *Phys. Rev. Lett.* **100** 060504
[8] Paesani S, Bulmer J F F, Jones A E, Santagati R and Laing A 2021 Scheme for universal high-dimensional quantum computation with linear optics *Phys. Rev. Lett.* **126** 230504
[9] Soltamov V A, Kasper C, Poshakinskiy A V, Anisimov A N, Mokhov E N, Sperlich A, Tarasenko S A, Baranov P G, Astakhov G V and Dyakonov V 2019 Excitation and coherent control of spin qudit modes in silicon carbide at room temperature *Nat. Commun.* **10** 1678
[10] Hrmo P, Wilhelm B, Gerster L, van Mourik M W, Huber M, Blatt R, Schindler P, Monz T and Ringbauer M 2023 Native qudit entanglement in a trapped ion quantum processor *Nat. Commun.* **14** 2242
[11] Leupold F M, Malinowski M, Zhang C, Negnevitsky V, Cabello A, Alonso J and Home J P 2018 Sustained state-independent quantum contextual correlations from a single ion *Phys. Rev. Lett.* **120** 180401
[12] Morvan A, Ramasesh V V, Blok M S, Kreikebaum J M, O'Brien K, Chen L, Mitchell B K, Naik R K, Santiago D I and Siddiqi I 2021 Qutrit randomized benchmarking *Phys. Rev. Lett.* **126** 210504
[13] Cervera-Lierta A, Krenn M, Aspuru-Guzik A and Galda A 2022 Experimental high-dimensional Greenberger-Horne-Zeilinger entanglement with superconducting transmon qutrits *Phys. Rev. Appl.* **17** 024062
[14] Luo K *et al* 2023 Experimental realization of two qutrits gate with tunable coupling in superconducting circuits *Phys. Rev. Lett.* **130** 030603
[15] Ding Y, Bacco D, Dalgaard K, Cai X, Zhou X, Rottwitt K and Oxenløwe L K 2017 High-dimensional quantum key distribution based on multicore fiber using silicon photonic integrated circuits *npj Quantum Inform.* **3** 25
[16] Doda M, Huber M, Murta G, Pivoluska M, Plesch M and Vlachou C 2021 Quantum key distribution overcoming extreme noise: simultaneous subspace coding using high-dimensional entanglement *Phys. Rev. Appl.* **15** 034003
[17] Bulla L *et al* 2023 Distribution of genuine high-dimensional entanglement over 10.2 km of noisy metropolitan atmosphere *Phys. Rev. A* **107** L050402
[18] Luo Y-H *et al* 2019 Quantum teleportation in high dimensions *Phys. Rev. Lett.* **123** 070505
[19] Hu X M *et al* 2020 Experimental high-dimensional quantum teleportation *Phys. Rev. Lett.* **125** 230501
[20] Zhang H *et al* 2022 Resource-efficient high-dimensional subspace teleportation with a quantum autoencoder *Sci. Adv.* **8** eabn9783
[21] Bechmann-Pasquinucci H and Peres A 2000 Quantum cryptography with 3-state systems *Phys. Rev. Lett.* **85** 3313
[22] Campbell E T 2014 Enhanced fault-tolerant quantum computing in d-level systems *Phys. Rev. Lett.* **113** 230501
[23] Krishna A and Tillich J-P 2019 Towards low overhead magic state distillation *Phys. Rev. Lett.* **123** 070507
[24] Imany P, Jaramillo-Villegas J A, Alshaykh M S, Lukens J M, Odele O D, Moore A J, Leaird D E, Qi M and Weiner A M 2019 High-dimensional optical quantum logic in large operational spaces *npj Quantum Inform.* **5** 59
[25] Gao X, Erhard M, Zeilinger A and Krenn M 2020 Computer-inspired concept for high-dimensional multipartite quantum gates *Phys. Rev. Lett.* **125** 050501
[26] Daboul J, Wang X and Sanders B C 2003 Quantum gates on hybrid qudits *J. Phys. A: Math. Gen.* **36** 2525
[27] Klimov A B, Guzmán R, Retamal J C and Saavedra C 2003 Qutrit quantum computer with trapped ions *Phys. Rev. A* **67** 062313
[28] Howard M and Vala J 2012 Qudit versions of the qubit $\pi/8$ gate *Phys. Rev. A* **86** 022316
[29] Babazadeh A, Erhard M, Wang F, Malik M, Nouroozi R, Krenn M and Zeilinger A 2017 High-dimensional single-photon quantum gates: concepts and experiments *Phys. Rev. Lett.* **119** 180510
[30] Gao X, Krenn M, Kysela J and Zeilinger A 2019 Arbitrary *d*-dimensional Pauli *X* gates of a flying qudit *Phys. Rev. A* **99** 023825
[31] Wang Y, Ru S, Wang F, Zhang P and Li F 2022 Experimental demonstration of efficient high-dimensional quantum gates with orbital angular momentum *Quantum Sci. Technol.* **7** 015016
[32] Su Q-P, Zhang Y, Bin L and Yang C-P 2022 Hybrid controlled-sum gate with one superconducting qutrit and one cat-state qutrit and application in hybrid entangled state preparation *Phys. Rev. A* **105** 042434
[33] Meng Z, Liu W-Q, Song B-W, Wang X-Y, Zhang A-N and Yin Z-Q 2024 Experimental realization of high-dimensional quantum gates with ultrahigh fidelity and efficiency *Phys. Rev. A* **109** 022612
[34] Lanyon B P, Barbieri M, Almeida M P, Jennewein T, Ralph T C, Resch K J, Pryde G J, O'Brien J L, Gilchrist A and White A G 2009 Simplifying quantum logic using higher-dimensional Hilbert spaces *Nat. Phys.* **5** 134
[35] Fedorov A, Steffen L, Baur M, da Silva M P and Wallraff A 2012 Implementation of a Toffoli gate with superconducting circuits *Nature* **481** 170
[36] Liu W-Q, Wei H-R and Kwek L-C 2020 Low-cost Fredkin gate with auxiliary space *Phys. Rev. Appl.* **14** 054057
[37] Gao X, Appel P, Friis N, Ringbauer M and Huber M 2023 On the role of entanglement in qudit-based circuit compression *Quantum* **7** 1141
[38] Li W-D, Gu Y-J, Liu K, Lee Y-H and Zhang Y-Z 2013 Efficient universal quantum computation with auxiliary Hilbert space *Phys. Rev. A* **88** 034303
[39] Barenco A, Bennett C H, Cleve R, DiVincenzo D P, Margolus N, Shor P, Sleator T, Smolin J A and Weinfurter H 1995 Elementary gates for quantum computation *Phys. Rev. A* **52** 3457
[40] Brylinski J L and Brylinski R 2001 arXiv:quant-ph/0108062
[41] Di Y-M and Wei H-R 2013 Synthesis of multivalued quantum logic circuits by elementary gates *Phys. Rev. A* **87** 012325
[42] Brennen G K, Bullock S S and O'Leary D P 2006 Efficient circuits for exact-universal computations with qudits *Quantum Inf. Comput.* **6** 436
[43] Jiang G-L, Liu W-Q and Wei H-R 2024 Optimal quantum circuits for general multi-qutrit quantum computation *Adv. Quantum Technol.* **7** 2400033
[44] Di Y-M and Wei H-R 2015 Optimal synthesis of multivalued quantum circuits *Phys. Rev. A* **92** 062317
[45] Nakajima Y, Kawano Y, Sekigawa H, Nakanishi M, Yamashita S and Nakashima Y 2009 Synthesis of quantum circuits for *d*-level systems by using cosine-sine decomposition *Quantum Inf. Comput.* **9** 423
[46] Bullock S S, O'Leary D P and Brennen G K 2005 Asymptotically optimal quantum circuits for *d*-level systems *Phys. Rev. Lett.* **94** 230502

[47] Mansky M B, Castillo S L, Puigvert V R and Linnhoff-Popien C 2023 Near-optimal quantum circuit construction via Cartan decomposition *Phys. Rev. A* **108** 052607
[48] Shende V V, Markov I L and Bullock S S 2004 Minimal universal two-qubit controlled-NOT-based circuits *Phys. Rev. A* **69** 062321
[49] Shende V V, Bullock S S and Markov I L 2006 Synthesis of quantum-logic circuits *IEEE Trans. CAD* **25** 1000
[50] Reck M, Zeilinger A, Bernstein H J and Bertani P 1994 Experimental realization of any discrete unitary operator *Phys. Rev. Lett.* **73** 58
[51] Clements W R, Humphreys P C, Metcalf B J, Kolthammer W S and Walsmley I A 2016 Optimal design for universal multiport interferometers *Optica* **3** 1460
[52] Meng H 2022 Deterministic linear-optical quantum control gates utilizing path and polarization degrees of freedom *Phys. Rev. A* **105** 032607
[53] Paige C C and Wei M 1994 History and generality of the CS decomposition *Linear Algebra Appl.* **208–9** 303
[54] Brennen G K, O'Leary D P and Bullock S S 2005 Criteria for exact qudit universality *Phys. Rev. A* **71** 052318